Paleobiology, 47(4), 2021, pp. 612–631
DOI: 10.1017/pab.2021.9

PALEOBIOLOGY
A PUBLICATION OF THE Paleontological SOCIETY

Article

Reconstructing dietary ecology of extinct strepsirrhines (Primates, Mammalia) with new approaches for characterizing and analyzing tooth shape

Ethan L. Fulwood, Shan Shan, Julia M. Winchester, Tingran Gao, Henry Kirveslahti, Ingrid Daubechies, and Doug M. Boyer*

Abstract.—The morphological and ecological diversity of lemurs and lorisiformes once rivaled that of the rest of the primate order. Here, we assemble a dataset of 3D models representing the second mandibular molars of a wide range of extant and fossil strepsirrhines encompassing this diversity. We use these models to distill quantitative descriptors of tooth form and then analyze these data using new analytical methods. We employ a recently developed dental topography metric (ariaDNE), which is less sensitive to details of random error in 3D model quality than previously used metrics (e.g., DNE); Bayesian multinomial modeling with metrics designed to measure overfitting risk; and a tooth segmentation algorithm that allows the shapes of disaggregated tooth surface features to be quantified using dental topography metrics. This approach is successful at reclassifying extant strepsirrhine primates to known dietary ecology and indicates that the averaging of morphological information across the tooth surface does not interfere with the ability of dental topography metrics to predict dietary adaptation. When the most informative combination of dental topography metrics is applied to extinct species, many subfossil lemurs and the most basal fossil strepsirrhines are predicted to have been primarily frugivorous or gummivorous. This supports an ecological contraction among the extant lemurs and the importance of frugivory in the origins of crown Strepsirrhini, potentially to avoid competition with more insectivorous and folivorous members of Paleogene Afro-Arabian primate faunas.

Ethan L. Fulwood[†]. Department of Neuroscience, Washington University in St. Louis School of Medicine, St. Louis, Missouri 63110, U.S.A.; and Department of Evolutionary Anthropology, Duke University, Durham, North Carolina 27708, U.S.A. E-mail: ethanfulwood@upike.edu [†]Present address: Kentucky College of Osteopathic Medicine, Pikeville, Kentucky 41501, U.S.A.

Shan Shan[‡] and Ingrid Daubechies. Department of Mathematics, Duke University, Durham, North Carolina 27708 U.S.A. [‡]Present address: Department of Mathematics and Statistics, Mt. Holyoke College, South Hadley, Massachusetts 01075, U.S.A.

Julia M. Winchester and Doug M. Boyer. Department of Evolutionary Anthropology, Duke University, Durham, North Carolina 27708, U.S.A.

Tingran Gao. Department of Statistics, University of Chicago, Chicago, Illinois 60637, U.S.A.

Henry Kirveslahti. Department of Statistical Science, Duke University, Durham, North Carolina 27708, U.S.A.

Accepted: 27 January 2021
*Corresponding author.

Introduction

Precisely occluding heterodont dentition unlocked a range of efficient food-processing strategies, selecting for a close fit between fine aspects of tooth shape and dietary strategy in mammals (Simpson 1933; Crompton 1970; Ungar 2010; Bhullar et al. 2019). Tooth shape is expected to vary with the material properties of the plant and animal parts that mammals exploit for food (Yamashita 1998; Lucas 2004; Ungar 2007, 2010). Most attempts to link tooth shape to dietary adaptation have focused on the molars and premolars, as incisors and canines are under selection to facilitate ingestion of food items that may relate more to geometry or propensity for escape than to food material properties, and also for sociosexual functions (Kay 1975, 1977; Kay and Hylander 1978; Kay and Simons 1980; Kay and Covert 1984; Kay and Ungar 1997; Yamashita 1998,

2003; Lucas 2004; Boyer 2008; Bunn and Ungar 2009; Ungar 2010; Bunn et al. 2011; Winchester et al. 2014; Allen et al. 2015; López-Torres et al. 2017; Pineda-Munoz et al. 2017; Selig et al. 2019).

Molar Shape and Dietary Adaptation.—Descriptive studies of tooth shape have long linked the qualitative form of the mammalian molar to aspects of diet (Gregory 1922; Simpson 1933; Crompton 1970). Quantitative approaches for describing the occlusal surface of teeth have taken two contrasting approaches: shearing metrics and dental topography metrics. Shearing quotients (SQ) and shearing ratios (SR) disaggregate and measure features on the tooth surface related to "shearing" or, more generally, food fragmentation, achieved through the interaction of blades on the tooth surface (Kay 1975, 1978; Kay and Covert 1984; Yamashita 1998; Lucas 2004). SQ and SR are measured as the sum of the lengths of the shearing structures of a tooth normalized to tooth length. This measurement appears to reflect the proportion of structural carbohydrates in the diets of primates and is effective in distinguishing folivores and insectivores from frugivores (Kay and Covert 1984). Folivores and insectivores resemble one another in shearing capacity, however, and must be distinguished using body size (Kay 1975; Kay and Covert 1984).

Comparisons using SQ and SR require the identification of homologous shearing structures across a sample of different taxa, which makes some contrasts impossible and others misleading if comparing teeth with different fundamental geometries (Kay and Simons 1980; Kay and Ungar 1997). SQ and SR also cannot characterize many other potentially adaptive features of the occlusal surface, including tooth height, tooth surface complexity, or the projection of sharp cusps (Ungar and Williamson 2000).

Dental topography metrics are designed to address these issues by abstracting functional information from a continuous occlusal surface. Dental topography metrics have the advantages over shearing metrics of (1) incorporating additional potentially relevant functional information, (2) ease of automation for the analysis of large samples, and (3) diminished reliance on the identification of homologous structures upon comparison among phylogenetically disparate taxa (Ungar and Williamson 2000; Boyer 2008; Bunn et al. 2011; Winchester et al. 2014; Winchester 2016). Whole occlusal surfaces may also have "emergent" functional properties that result from the interaction of multiple surface features and would not be captured by discretizing measurements of tooth surface structures (Winchester 2016).

Three dental topography metrics have been extensively applied to reconstruct dietary ecology in primates: relief index (RFI), Dirichlet normal energy (DNE), and orientation patch count (OPC). RFI measures crown relief, or the projection of the occlusal surface into space, a straightforward method of describing the functional surface available for processing food. RFI quantifies occlusal relief using a ratio of the area of the crown surface ("3D" area) to the cross-sectional area of the tooth footprint (Ungar and Williamson 2000; Boyer 2008). Crown surface can be measured from the lowest point of the talonid basin (sensu Ungar and Williamson 2000) or from the enamel–cementum junction (sensu Boyer 2008). RFI is expected to correlate with SQ and SR, as both capture the elaboration of occlusal features used to process structural carbohydrates (Boyer 2008; Bunn et al. 2011). However, in capturing the projection of the tooth into space without regard for the identity of individual tooth features, it is less sensitive to questions of homology. In capturing the walls of the tooth crown, RFI sensu Boyer (2008) also measures hypsodonty, important as an adaptation to resist attritional agents found in many plant tissues (Fortelius et al. 2002; Jardine et al. 2012).

DNE measures the curvature of the occlusal surface as deviation in normal "energy" from a plane (Bunn et al. 2011; Winchester 2016; Shan et al. 2019). Dirichlet's energy is used by mathematicians to describe the variability of a function (Spagnolo 1976). DNE applies this energy calculation approach to a digitized tooth surface. DNE is measured as a sum of the energies describing the change in orientation of mesh polygon "normal vector" (a line perpendicular to the polygon face) across a surface. DNE and RFI both capture tooth

https://doi.org/10.1017/pab.2021.9 Published online by Cambridge University Press

sharpness, which, like shearing crest length, is associated with the processing of tough structural carbohydrates. DNE, however, may be relatively less affected by wear than SQ, SR, and RFI, and can be calculated on digital surfaces independent of the orientation of the tooth, a major advantage in automating the analysis of large numbers of specimens (Bunn et al. 2011).

Mesh analysis methods, especially DNE, are sensitive to details of mesh quality and preparation, especially the number of mesh vertices and the iterative application of smoothing algorithms (Spradley et al. 2017; Berthaume et al. 2019). A recently described implementation of DNE, "ariaDNE," was developed to address these issues, allowing for comparisons among studies and concatenation of larger datasets (Shan et al. 2019). This metric is calculated by integrating measurements of the vertex-by-vertex normal energies of meshes over local "bandwidths," which capture tooth surface features at different resolutions. Lower bandwidths capture smaller tooth surface features, which may or may not reflect functional adaptations of teeth. The sum of ariaDNE values calculated for each vertex is comparable to the DNE of Bunn et al. (2011), which was designed principally to describe tooth sharpness. The variance of vertex-by-vertex ariaDNE across the surface can also be calculated, which may capture some aspects of the distribution of sharp and flat features on a tooth surface. The ability of ariaDNE to reclassify a limited number of platyrrhine teeth to genus has been examined (Shan et al. 2019), but correlation between these metrics and dietary ecology has not been examined in a large primate sample like that used in the validation of DNE sensu Bunn et al. (2011).

Shearing metrics, RFI, and DNE measure the shape of the tooth surface as a correlate of a tooth's projection into space. OPC is distinctive in measuring the complexity of a tooth surface as a count of slopes sharing a single aspect (Evans et al. 2007; Evans and Jernvall 2009; Evans 2013; Pineda-Munoz et al. 2017; Evans and Pineda-Munoz 2018). The calculation of OPC proceeds by first identifying regions of a digital model sharing a slope of the same orientation in one of a set number of cardinal directions (typically eight). The number of "patches" of cells sharing slopes of the same orientation is then counted. A simple tooth like the carnassial of a hypercarnivore will have a relatively low OPC, while a tooth with many intersecting crests and cusps or, alternatively, a tooth with a high degree of enamel crenulation will have more patches, yielding a higher score. OPC attempts to quantify the "number of tools" present on a dental surface, which makes it unique as a topography metric, most of which describe the "shape of the tools" (Evans et al. 2007).

Much of the promise of quantitative descriptors of tooth shape lies in their potential application to the fossil record. Application to fossil organisms requires descriptors to be validated on a sample of extant taxa of known dietary ecology. Primates have been a major focus of these studies since the first description of SQ, partially because of a persistent interest in the fossil record of primates and partially because of their subtly distinct but relatively well-studied dietary ecologies (Kay 1975). Studies reconstructing diet in fossil organisms generally recommend combining multiple shape descriptors (an approach referred to as "multiproxy dental morphology analysis" by Pineda-Munoz et al. [2017]), as this consistently improves model reclassification rates, particularly when using linear discriminant function analysis (DFA), by improving model fit (Bunn et al. 2011; Winchester et al. 2014; Allen et al. 2015; Pineda-Munoz et al. 2017). However, the addition of model parameters introduces the danger of overfitting by allowing models to learn too much from the in-sample dataset. Overfitting compromises out-of-sample prediction by modeling noise in the multidimensional distribution of tooth shape parameters in addition to any biological signal. Bayesian approaches to parameter regularization and model comparison can combat overfitting (McElreath 2015) but have not previously been applied to tests of the relationship between tooth shape and dietary ecology.

Disaggregating Adaptation in Tooth Surface Features.—The ability of mesh analysis methods to capture the shape of an entire tooth surface is both a strength and a weakness, as disaggregated regions of the tooth surface may play distinct functional roles that dental

https://doi.org/10.1017/pab.2021.9 Published online by Cambridge University Press

topography metrics have the potential to "average" away (Allen et al. 2015). Individual shearing crests and crushing basins may play particular roles in food fracture or in constraining the movements of the lower jaw in space as it comes into occlusion (Simpson 1933; Kay and Hiiemae 1974; Kay 1975, 1977; Sheine and Kay 1982). Past work testing these hypotheses has used approximations of areas and shapes derived from linear measurements of tooth surface features (Kay and Hiiemae 1974; Kay 1975; Sheine and Kay 1982; Allen et al. 2015). Newly developed shape-segmentation methods introduced here allow the shapes of regions of the tooth surface to be analyzed quantitatively using the dental topographic approaches employed on whole-tooth surfaces. Metrics using the ariaDNE implementation of DNE are particularly appropriate for this analytical approach, as they are orientation invariant and show less sensitivity to variation in mesh face count than other dental topography metrics (Shan et al. 2019).

Objectives.—The goals of this paper are twofold. First, combinations of dental topography metrics, including ariaDNE and Bayesian fitting approaches, are validated on a sample of extant strepsirrhine primates. This builds on the description of ariaDNE and instructions for use presented in Shan et al. (2019). Second, high-performing combinations of metrics are applied to fossil and subfossil strepsirrhines to better understand strepsirrhine dietary evolution, particularly in the context of lemur origins.

A series of tests are first run on the extant strepsirrhine dataset. The dietary reclassification utility of the recent ariaDNE implementation of DNE, both summed across vertices and as a coefficient of variation of vertex-by-vertex values across the surface, is assessed on a sample of second lower molars from extant strepsirrhine primates. Bayesian models are constructed using regularizing priors, and model comparison metrics are used to address the potential for overfitting when combining ariaDNE with the additional dental topography metrics RFI and OPC. Finally, six bandwidths of ariaDNE averaging are compared to determine the highest performing in dietary reclassification. Dietary signal from disaggregated second lower molar segments is also investigated. If individual tooth structures are under relatively independent selection for function in food processing, then the dietary signal of aggregated tooth segment shapes should be higher than that of tooth surfaces considered as a single mesh (Allen et al. 2015).

High-performing combinations of dental topography metrics are then used to reconstruct the dietary ecology of seven fossil strepsirrhine taxa from the Tertiary of Africa and Asia and specimens representing seven recently extinct lemur genera, known only from subfossils. These reconstructions are compared to existing understandings of the dietary ecology of these taxa, derived from descriptive analyses of tooth shape, the calculation of shearing quotients, and dental microwear (Jungers et al. 2002; Godfrey et al. 2004, 2006, 2012; Marivaux et al. 2013).

Fossil taxa include the stem strepsirrhine *Djebelemur martinezi*; the fossil lorisiforms *Karanisia clarki*, *Komba robustus*, *Nycticeboides simpsoni*, and *Wadilemur elegans*; and the fossil chiromyiform lemurs *Plesiopithecus teras* and *Propotto leakyi*. Of these taxa, previous studies have quantitatively assessed diet preference in *D. martinezi*, *K. clarki*, *P. teras*, and *W. elegans*. *Djebelemur martinezi* has been reconstructed as primarily insectivorous using shearing quotients and dental microwear (Marivaux et al. 2013). Shearing quotients and body-size reconstructions have reconstructed *P. teras* as frugivorous and *K. clarki* and *W. elegans* as frugivorous and insectivorous (Kirk and Simons 2000; Marivaux et al. 2013). *Karanisia clarki* was also classified as an omnivore in the dental topographic analysis of Patel et al. (2017), a result consistent with frugivory/insectivory. López-Torres et al. (2020) report evidence from the distribution of enamel in the anterior dentition of *K. clarki* that it consumed a significant amount of tree exudates and should be thought of as an obligate gummivore. Qualitative arguments have been advanced for an insectivorous diet in *K. robustus* and for a diet consisting primarily of fruit (or at least not of leaves) in *N. simpsoni* and *P. leakyi* (Walker 1969; MacPhee and Jacobs 1986; McCrossin 1992).

The recently extinct subfossil lemurs represent a diverse fauna, and dental

https://doi.org/10.1017/pab.2021.9 Published online by Cambridge University Press

microwear, shearing quotients, and dental topography metrics have all been applied to reconstructing their dietary ecologies (Jungers et al. 2002; Godfrey et al. 2004, 2006, 2012). The sample examined here includes individuals from the extinct families Archaeolemuridae (*Archaeolemur* and *Hadropithecus*), Palaeopropithecidae (*Babakotia*, *Mesopropithecus*, *Palaeopropithecus*) and Megaladapidae (*Megaladapis*), and the genus *Pachylemur* in the family Lemuridae. Palaeopropithecids and *Megaladapis* appear to have been primarily folivorous, while *Pachylemur* shared a primarily frugivorous diet with its extant lemurid relatives (Godfrey 2017). The archaeolemurids show an unusual dental morphology most like that of some cercopithecoid monkeys and suggesting a diet requiring frequent hard-object processing (Godfrey et al. 2005, 2016).

Methods

Sample.—Metrics were calculated on digitized scans of 218 second lower molars from 40 extant strepsirrhine species representing 22 genera. Specimens were drawn from every lemur genus but the rare hairy-eared dwarf lemur *Allocebus* and the adaptively unusual aye-aye *Daubentonia*, whose molar morphology is unlikely to reflect its diet of defended grubs and fruits, and from every lorisiform genus but the recently erected *Paragalago* (Masters et al. 2017) (Supplementary Table 1). The sample builds on tooth scans compiled by Bunn et al. (2011) and is processed using a similar protocol. Mesh ".ply" surfaces were produced from microcomputed tomography (microCT) scans of osteological specimens or epoxy casts made from polyvinylsiloxene molds using proprietary segmenting and smoothing functions in Avizo (v. 8) to facilitate cropping using the natural contour of the tooth crown (Visualization Sciences Group, Burlington, Mass., USA). The second lower molar was cropped from each mesh at the enamel–cementum junction using Geomagic (3D Systems, Rock Hill, S.C., USA), and individual teeth were simplified to 10,000 faces and smoothed over 20 iterations using smoothing functions in Avizo. Smoothing was kept to 20 iterations at each step to avoid the introduction of mesh irregularities at higher numbers of iterations (Spradley et al. 2017). Teeth that showed minimal wear were selected a priori. However, distributions of calculated values were also examined post hoc, and teeth that were significant outliers and visibly more worn than other specimens in the sample for each taxon were then excluded (one specimen of *Arctocebus*, one specimen of *Euoticus*, one specimen of *Lepilemur*, three specimens of *Microcebus*, one specimen of *Prolemur*, and one specimen of *Propithecus*).

Three dietary categories were used, with taxa assigned to each category based on data on the proportional representation of foods from each category in diets observed in studies of wild populations (Charles-Dominique 1977, 1979; Hladik 1979; Bearder and Martin 1980; Hladik et al. 1980; Ganzhorn et al. 1985; Harcourt 1986, 1991; Harcourt and Nash 1986; Nash 1986; Masters et al. 1988; Overdorff 1992; Sterling et al. 1994; Hemingway 1996; Overdorff et al. 1997; Balko 1998; Fietz and Ganzhorn 1999; Vasey 2000, 2002; Thalmann 2001; Britt et al. 2002; Nekaris and Rasmussen 2003; Powzyk and Mowry 2003; Streicher 2004, 2009; Nekaris 2005; Gould 2006; Norscia et al. 2006; Wiens et al. 2006; Lahann 2007; Dammhahn and Kappeler 2008; Burrows and Nash 2010; Olson et al. 2013; Rode-Margono et al. 2014; Sato et al. 2016; Erhart et al. 2018). If members of a genus consumed the greatest component of their diet from leaves or insects, the genus was classified as folivorous or insectivorous, respectively. Taxa that consumed the greatest part of their diet from fruits, gums, and other plant reproductive structures were classified as frugivorous (Supplementary Table 1).

Dental Topography Metrics.—Functional tooth shape was quantified using the dental topography metrics DNE, RFI, and OPC. DNE was calculated both sensu Bunn et al. (2011) using the R package molaR (Pampush et al. 2016b) and as ariaDNE using functions in MATLAB (Shan et al. 2019). The sum of ariaDNE at each vertex and its coefficient of variation (CV) across the tooth surface (here called ariaDNE and ariaDNE CV, respectively) were each calculated. RFI was calculated using the open-source stand-alone program Morphotester (Winchester 2016). RFI calculation on one specimen of *Varecia variegata* (USNM 84383)

https://doi.org/10.1017/pab.2021.9 Published online by Cambridge University Press

failed in Morphotester and was performed using molaR. OPC was calculated using the "orientation patch count rotated (OPCR)" approach implemented in molaR. OPCR accounts for deviation in the orientation of the tooth on the *x*,*y* plane by averaging the counts calculated over 45° rotations (Evans and Jernvall 2009). OPCR was calculated using 3D-OPCR functions, which differs from the DEM-OPCR approach taken by previous studies examining large samples of strepsirrhine primates (Bunn et al. 2011; Winchester et al. 2014). 3D-OPCR calculates OPCR from the orientation of the polygons directly, without first converting the occlusal topography into a digital elevation model (DEM), and appears to better reflect the complexity of tooth surface features (Winchester 2016). Variables were transformed to z-scores before analysis through the division of each data point by the sample standard deviation and the subtraction of the sample mean of each variable in order to correct for differences in the scale of each variable and to improve model fit.

Shape Segmentation.—Each tooth in the sample was segmented into 15 regions using the hecate MATLAB package. This algorithm automatically identifies corresponding shape regions across all tooth surfaces in a consistent manner, using high-quality point-to-point mappings between all pairs of surfaces. These regions represent parts of the tooth that vary together across a given tooth sample and are intended to correspond to the sorts of structures commonly identified and named by morphologists, such as cusps and crests.

The algorithms implemented in hecate can be summarized in three phases. First, continuous Procrustes distances (Al-Aifari et al. 2013) are calculated between all pairs of sample meshes, using whole-surface meshes instead of sequences of landmarks as described in Gao et al. (2018). The distances computed characterize pairwise (dis-)similarity among all surfaces by minimizing an energy function over all admissible maps between two disk-type surfaces, thus leading to an energy-minimizing point-to-point correspondence map associated with the distance value. Because the computations at this stage are all carried out in a pairwise manner, these point-to-point correspondence maps are generally not transitive. Next, the pairwise distances and their associated correspondence maps are assembled into a large-scale "random walk" modeling how a hypothetical "particle" would travel from tooth surface to tooth surface following the guidance of the correspondence maps; such a probabilistic model is known as a *horizontal random walk* (Gao 2015, 2021). Intuitively, when the particle is constrained to hop within similar surfaces (with small pairwise distance), the particle will slowly drift in position but mostly remain within corresponding regions of local geometric similarity; in contrast, when jumping across highly dissimilar surfaces (with large pairwise distance), the particle will quickly deviate from its regular routine and become visible all over any single tooth surface in the sample.

hecate leverages this phenomenon to identify corresponding regions across tooth surfaces by constructing a *horizontal random walk matrix* encoding the transition probability from each vertex on a triangular mesh to vertices on other triangular meshes, computed from the continuous Procrustes distance and the correspondence maps. Finally, eigen-decomposition of this horizontal random walk matrix provides a way to embed all tooth surfaces into a common "template" in the spectral domain. In this spectral representation, the tooth surfaces are all registered onto a virtual "common domain" to provide a basis for transitive, consistent comparisons across all surfaces in the sample. Machine learning techniques such as *k*-means clustering can then be applied to this spectral representation; the *k* groups of point clouds in the spectral domain can be mapped back to corresponding regions on the tooth surfaces, generating consistent segments across all surfaces.

The entire algorithmic workflow is integrated into the MATLAB software package hecate. This package takes as an input a set of meshes of whole teeth and outputs *n* mesh files, representing the number (*n*) of segments requested by the user. Input mesh files do not require processing beyond the "cleaning" routinely done in studies of dental topography (Winchester et al. 2014). These mesh files can then be analyzed using orientation-invariant dental topography metrics like DNE. Metrics that rely on meshes sharing a consistent orientation can be misleading,

https://doi.org/10.1017/pab.2021.9 Published online by Cambridge University Press

however, as these meshes are oriented according to their positions in the teeth from which they have been segmented. Downloads of scripts to implement hecate in MATLAB and additional documentation are available from Winchester (2020).

Dietary Signal and Dental Topography Metrics.—The reclassification utility of ariaDNE implementations of DNE in combination with other dental topography metrics was assessed and compared with earlier implementations of DNE using the extant strepsirrhine sample in both DFA and multinomial modeling paradigms. Models were constructed using each of six bandwidths of ariaDNE and DNE sensu Bunn et al. (2011) combined with RFI and OPC, creating models of nested complexity.

First, reclassification success rates from a cross-validated ("leave-one-out") DFA was performed using the package MASS in R. Successful reclassifications of genera using genus mean values for each dental topography metric and the average successful reclassifications of the specimens within each genus are both reported from the DFA.

Second, likelihood of membership in each of the three dietary categories was modeled in a Bayesian, multilevel framework using functions in the R packages brms and the Stan engine (Bürkner 2017). Four chains were run over 3000 iterations, with a 1000-iteration warm-up. Chain convergence was assessed using the rhat parameter, the number of effective samples returned, and visual inspection of the chain trace plots. Bayesian, multilevel methods, which have not previously been applied to dietary classification from dental topography metrics, were chosen to complement a more traditional linear discriminant analysis approach for two broad reasons. First, they allow for clustering in the data to be modeled as group-specific intercepts, which is useful for analyzing multiple specimens from single taxa or multiple segmented regions from a single molar, and for the joint modeling of phylogenetic covariance among taxa. Second, through the use of regularizing priors and model comparison metrics, they allow the explicit minimization and measurement of overfitting risk.

Models were constructed using the software default 0.8 bandwidth of ariaDNE, which, as discussed in the "Results," was the highest performing in DFA. ariaDNE bandwidths correspond to the degree of local averaging around each vertex. For each vertex, the calculation of ariaDNE assigns a weight to the rest of the points in the mesh that is proportionate to the inverse square of the bandwidth value. Each bandwidth expresses a length of the same units as the distance between any two vertices in the mesh (Shan et al. 2019).

ariaDNE values were combined variously with ariaDNE 0.8 CV, RFI, and OPC in models of nested complexity using a sample of individual tooth specimens; in a multilevel framework with different slopes for each genus; and in a multilevel framework that incorporates phylogenetic covariance among genera using a consensus phylogeny from Herrera and Dávalos (2016). Phylogenetic covariance is modeled in brms using a phylogenetic mixed modeling approach that jointly estimates and incorporates phylogenetic signal into the strength of the covariance relationships (Housworth et al. 2004). The estimated phylogenetic signal can be reported as the proportion of the variance explained by the modeled covariance and is analogous to Pagel's lambda metric (Housworth et al. 2004; Bürkner 2020). Models of different complexity were compared using the "Pareto-Smoothed importance sampling leave-one-out cross validation" approximation (LOOIS) implemented in the loo package in R and accessed through brms (Vehtari et al. 2017). This metric efficiently approximates a model's leave-one-out reclassification success. This allows the measurement of overfitting risk, which reflects the ability of a model to predict out-of-sample outcomes, an important consideration in models generated for application to the fossil record.

Dietary Signal in the Segmented Molar.—ariaDNE values (at the 0.08 bandwidth of local averaging) were calculated on the sample of second lower molars segmented using the hecate method. Categorical multilevel models were constructed in a Bayesian framework, with specimens in each genus permitted to share independent intercepts. Two partitions of the data were considered. The likelihood of

https://doi.org/10.1017/pab.2021.9 Published online by Cambridge University Press

membership in each dietary category was modeled as a function of the shapes of each segment, with each tooth permitted to have an independent intercept and each class of segments permitted to share an independent intercept and slope. Likelihoods were also modeled using ariaDNE values calculated for each continuous surface. ariaDNE was used as a metric because it can be compared among surfaces, such as those of tooth segments with different areas, which differ in mesh face count (Shan et al. 2019). Models were constructed to account for the clustering of specimens within genus but did not incorporate phylogenetic covariance. Predictive models were compared using LOOIS (Vehtari et al. 2017).

Reconstructed Dietary Ecology in Fossil Strepsirrhines and Subfossil Lemurs.—Two approaches were taken to reconstruct dietary ecology in the extinct strepsirrhine sample. DFA models were constructed using genus mean data ("genus DFA") and specimen-level data, with the mean reconstructed probability of membership in each dietary category among all of the individual specimens reported for each genus ("specimen DFA"). DFA modeling used the combination of variables that were the highest performing in reclassifying extant taxa using DFA leave-one-out cross validation. A Bayesian multilevel model was also constructed incorporating the maximally informative combination of variables that reported an acceptable ($k < 0.7$) overfitting risk as determined through LOOIS comparisons (k representing a parameter of the pareto fit to the importance ratios of each leave-one-out model). This model incorporates specimen-level clustering within genera by allowing each genus an independent intercept. Each extant taxon was stripped of information about its dietary ecology and classified to dietary ecology iteratively using the same approach. This allows the classifications of extinct taxa to be contextualized using informationally analogous reclassifications of extant taxa of known diet.

Institutional Abbreviations.—CBI, Office National des Mines, Tunis, Tunisia; DLC/DPC, Division of Fossil Primates, Duke Lemur Center, Durham, N.C.; MCZ, Museum of Comparative Zoology, Harvard University, Cambridge Mass.; USNM, National Museum of Natural History, Smithsonian Institute, Washington, D.C.

Results

Dental Topography Metrics and Dietary Category.—Calculated values for the 0.08 bandwidth of ariaDNE and ariaDNE CV, OPC, and RFI for each genus are presented in Supplementary Table 2. At each bandwidth, ariaDNE was highest in insectivores and lowest in frugivores, while ariaDNE CV was highest in folivores and lowest in insectivores. DNE sensu Bunn et al. (2011) was highest in folivores and lowest in frugivores. OPC was also highest in folivores and lowest in frugivores. RFI was highest in insectivores and lowest in frugivores. Values for each dietary group overlapped at the upper and lower ends of their ranges, but means were separated by at least 1 SE for every metric (Supplementary Table 3).

Whole-Tooth Reclassification Success.—Implementations of ariaDNE showed the highest DFA reclassification success of all dental topography metrics (Table 1). The highest-performing combination of variables (ariaDNE sum and CV at the 0.08 bandwidth combined with RFI and OPC) reclassified strepsirrhine genera to the correct dietary ecology with 100% accuracy using genus means and with 86% accuracy when measured from the average reclassification success of the specimens within each genus. The position of each extant strepsirrhine genus on the two linear discriminant axes of a model combining ariaDNE 0.08, ariaDNE 0.08 CV, RFI, and OPC are presented in Figure 1. ariaDNE 0.08 is strongly correlated with the first linear discriminant axis (LD1) ($r^2 = 0.95$), ariaDNE 0.08 CV is strongly negatively correlated with LD2 ($r^2 = -0.94$); RFI is moderately correlated with LD1 ($r^2 = 0.55$), and OPC is moderately negatively correlated with LD2 ($r^2 = -0.60$).

Whole-Tooth Multinomial Modeling.—Chains from all models converged with a rhat of 1 and acceptable effective sample size (Supplementary Material). With each specimen treated as an independent data point, genus clustering accounted for, and phylogenetic covariance modeled, LOOIS preferred the combination of the 0.08 bandwidth of ariaDNE with its CV,

https://doi.org/10.1017/pab.2021.9 Published online by Cambridge University Press

TABLE 1. Reclassifications to dietary ecology in extant strepsirrhines using discriminant function analysis (DFA). Reclassification success using genus means is reported, with the average reclassification success of the specimens in each genus reported in parentheses. Rows indicate different bandwidths and columns different combinations of variables. DNE, Dirichlet normal energy; SD, coefficient of variation of DNE; RFI, relief index; OPC, orientation patch count.

	DNE	DNE + SD	DNE + SD + RFI	DNE + OPC	DNE + SD + OPC	DNE + SD + OPC + RFI
DNE sensu Bunn et al. 2011	0.55 (0.59)	NA	NA	0.82 (0.59)	NA	NA
ariaDNE 02	0.73 (0.64)	0.64 (0.68)	0.68 (0.68)	0.73 (0.68)	0.64 (0.73)	0.64 (0.68)
ariaDNE 04	0.77 (0.73)	0.68 (0.68)	0.77 (0.73)	0.73 (0.77)	0.73 (0.82)	0.68 (0.77)
ariaDNE 06	0.77 (0.73)	0.73 (0.86)	0.77 (0.91)	0.73 (0.82)	0.77 (0.82)	0.86 (0.77)
ariaDNE 08	0.68 (0.68)	0.86 (0.77)	0.95 (0.82)	0.77 (0.82)	0.82 (0.82)	100 (0.86)
ariaDNE 10	0.59 (0.59)	0.95 (0.82)	0.95 (0.82)	0.77 (0.82)	0.95 (0.86)	0.91 (0.86)
ariaDNE 12	0.68 (0.64)	0.91 (0.77)	0.95 (0.82)	0.86 (0.73)	0.82 (0.82)	0.86 (0.82)

OPC, and RFI ("all parameters model") (Table 2). Comparisons among data partitions preferred the model that clustered specimens by genus over the unclustered model and the model that included phylogenetic information. LOOIS preferences across alternate parameter combinations in the clustered and phylogenetic methods were mostly relatively small, however, and all combinations of variables were in the "good" or "ok" range ($k < 0.7$), with > 98% in the "good" range ($k < 0.5$). Because of this, the unclustered Bayesian model is

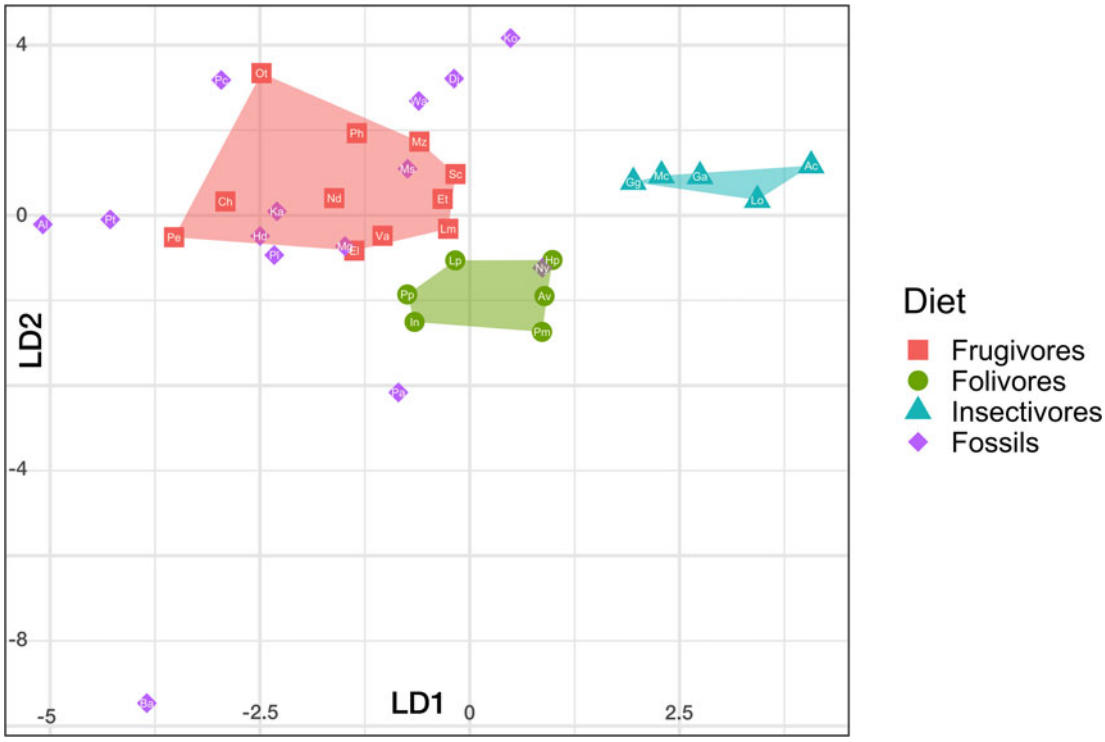

FIGURE 1. Plots of genus means along linear discriminant axes of discriminant function analysis (DFA). Model constructed using ariaDNE 0.08 with ariaDNE coefficient of variation (CV), relief index (RFI), and orientation patch count (OPC), including reconstructed subfossil lemurs. Ac, *Arctocebus*; Al, *Archaeolemur*; Av, *Avahi*; Ba, *Babakotia*; Ch, *Cheirogaleus*; Dj, *Djebelemur*; El, *Eulemur*; Et, *Euoticus*; Ga, *Galago*; Gg, *Galagoides*; Hd, *Hadropithecus*; Hp, *Hapalemur*; In, *Indri*; Ka, *Karanisia*; Ko, *Komba*; Lm, *Lemur*; Lo, *Loris*; Lp, *Lepilemur*; Mc, *Microcebus*; Mg, *Megaladapis*; Ms, *Mesopropithecus*; Mz, *Mirza*; Nd, *Nycticebus*; Ny, *Nycticeboides*; Ot, *Otolemur*; Pa, *Palaeopropithecus*; Pc, *Pachylemur*; Pe, *Perodicticus*; Ph, *Phaner*; Pl, *Plesiopithecus*; Pm, *Prolemur*; Pp, *Propithecus*; Pt, *Propotto*; Sc, *Sciurocheirus*; Va, *Varecia*; Wa, *Wadilemur*.

https://doi.org/10.1017/pab.2021.9 Published online by Cambridge University Press

TABLE 2. Comparisons among pareto-smoothed importance sampling leave-one-out cross validation approximation (LOOIS) information criteria calculated on models constructing using the 0.8 ariaDNE bandwidth. DNE, Dirichlet normal energy; CV, coefficient of variation of DNE; OPC, orientation patch count; RFI, relief index.

	Unclustered	Genus cluster	Phylogenetic cluster
DNE	341.4	297.7	308.1
DNE + CV	249.3	179.7	265.3
DNE + OPC	314.8	259.4	298.4
DNE + RFI	330.1	278.7	306.9
DNE + CV + OPC	237.1	167.5	257.0
DNE + CV + RFI	238.4	163.1	265.2
All metrics	226.6	151.8	257.0

discussed and figured below in order to explicate the influence of the dental topography metrics studied on the probability of membership in each diet group. This model is chosen because it demonstrates the same directional trends as more complex models, but with narrower probability intervals, making the trends clearer to visualize. Full model parameter estimates are included in the Supplementary Material. Coefficient values reported below represent the mean of the posterior distribution estimated by each model.

In the unclustered all parameters model, high ariaDNE values predict insectivorous diets (coefficient value predicting membership in category, relative to frugivory = 6.66); intermediate ariaDNE values predict folivorous diets (coefficient value predicting membership in category, relative to frugivory = 1.62); and low ariaDNE values predict frugivorous diets (Fig. 2). The molars of insectivorous strepsirrhines show the highest ariaDNE values, supporting this observation. High CV values predict folivorous diets (coefficient value predicting membership in category, relative to frugivory = 1.78); intermediate CV values predict frugivorous diets; and low CV values predict insectivorous diets (coefficient value predicting membership in category, relative to frugivory = −5.62). This reflects the concentration of folivorous taxa among the strepsirrhines with the highest ariaDNE CV values.

High OPC was positively predictive of folivory (coefficient value predicting membership in category, relative to frugivory = 0.79) and negatively predictive of insectivory (coefficient value predicting membership in category, relative to frugivory = −0.85) (Fig. 2). Conditional on the strong relationships with ariaDNE and ariaDNE CV, high RFI was actually negatively predictive of folivory (coefficient value predicting membership in category, relative to frugivory = −0.18) and insectivory (coefficient value predicting membership in category, relative to frugivory = −1.45), despite being absolutely higher in these groups than among frugivores.

Segmented Tooth Multinomial Modeling.—The hecate shape-segmentation algorithms were successful in isolating regions of local shape similarity corresponding to commonly identified cusps, crests, and basins (Fig. 3). However, models using the ariaDNE values of each segment performed no better in reclassification than models using ariaDNE summed across the tooth surface (LOOIS = −9.7 for whole-tooth model and −9.7 for segmented model) (Fig. 4). This indicates that the extra information provided by ariaDNE calculations on each segmented mesh did not improve dietary signal.

Classification of Extinct Strepsirrhines.—The dietary ecologies of extinct strepsirrhines were reconstructed using genus mean and specimen values in DFA and Bayesian multilevel models that included all parameters at the ariaDNE 0.8 bandwidth. Genus DFA and specimen DFA classifications are reported in Table 3. Means from the posterior probabilities of Bayesian model classifications included ariaDNE 0.08, ariaDNE CV 0.08, RFI, and OPC, and are reported in Table 4. In the DFA models, *Archaeolemur*, *Djebelemur*, *Karanisia*, *Megaladapis*, *Mesopropithecus*, *Hadropithecus*, *Pachylemur*, *Plesiopithecus*, *Propotto*, and *Wadilemur* were all reconstructed as frugivores; *Babakotia*, *Nycticeboides*, and *Palaeopropithecus* as folivores. *Komba* was reconstructed as frugivorous in the genus mean model and as insectivorous in the specimen classification model (Fig. 5). The Bayesian model differs from the genus mean DFA in classifying *Nycticeboides* as frugivorous and *Komba* as insectivorous (Tables 3, 4).

Discussion

The ariaDNE implementation of DNE has considerable value in describing dietary

https://doi.org/10.1017/pab.2021.9 Published online by Cambridge University Press

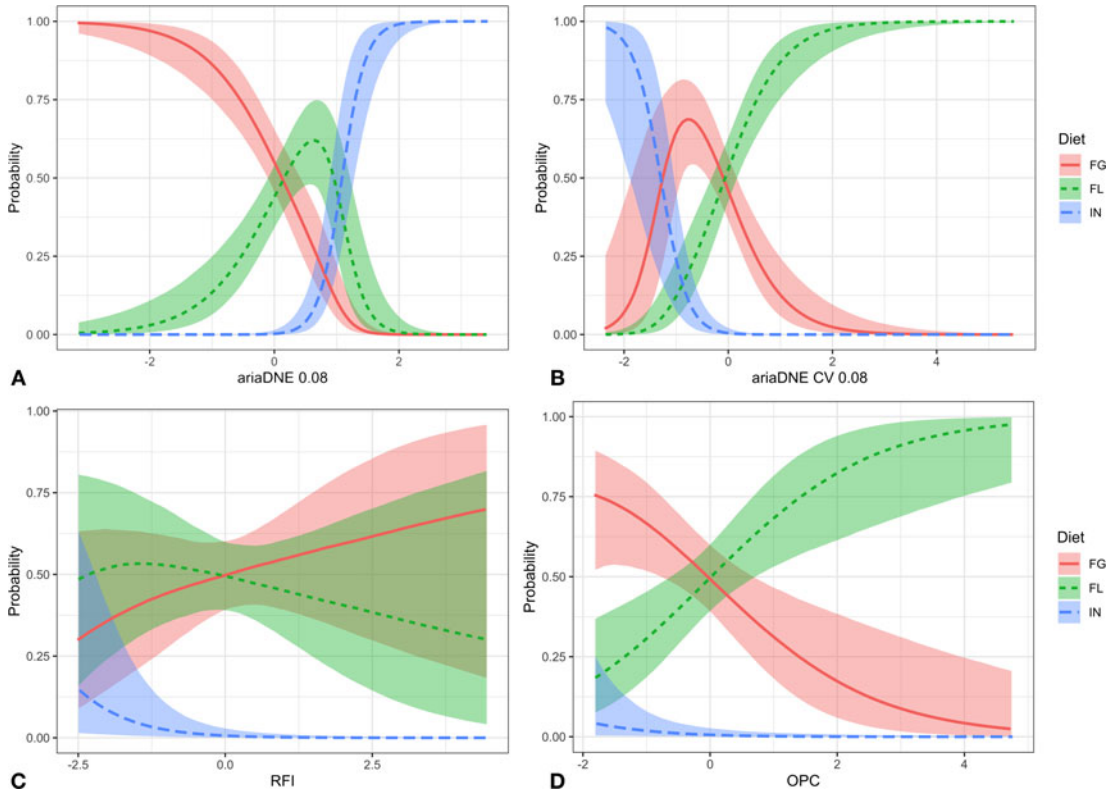

FIGURE 2. Relative probability of membership in each dietary category over the scaled range of values of ariaDNE bandwidth 0.08 estimated by multinomial Bayesian modeling (without including genus clustering or phylogenetic covariance) over the scaled range of values of A, ariaDNE; B, ariaDNE coefficient of variation (CV); C, relief index (RFI); D, orientation patch count (OPC). Shaded area represents consistency interval of middle 95% of the mass of the posterior distribution. FL, folivory; FG, frugivory; IN, insectivory.

ecology in strepsirrhines, particularly when using larger bandwidths of local averaging. At all bandwidths, ariaDNE outperforms traditional DNE in dietary reclassification. ariaDNE can be implemented in both DFA and Bayesian multinomial frameworks, and neither overfitting, when combined with additional metrics, nor averaging of functional information across the occlusal surface appears to represent major confounding factors. ariaDNE and ariaDNE CV used in combination add a valuable new dimension to dietary discrimination, particularly in distinguishing primate folivores from insectivores, a task that has traditionally proved difficult without the inclusion of additional body-size information.

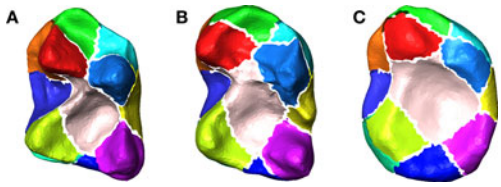

FIGURE 3. Regional segmentation of lower second molars created by hecate algorithms. A, *Arctocebus*; B, *Avahi*; C, *Cheirogaleus*.

Insectivorous teeth show surfaces with high average curvature across the surface, while folivores show moderate average curvature but high variability. Both insects and leaves require consumers to fragment relatively tough structural carbohydrates (Kay 1975; Lucas 2004; Ungar 2010). In leaves, structural carbohydrates are packaged within cellulose fibers and ligneous cell walls, while in insects they form the structural component of chitinous exoskeletons (Vincent 1990; Strait 1993; Strait and Vincent 1998; Lucas 2004). The common demands of these food materials explain the common elaboration of shearing crests and

https://doi.org/10.1017/pab.2021.9 Published online by Cambridge University Press

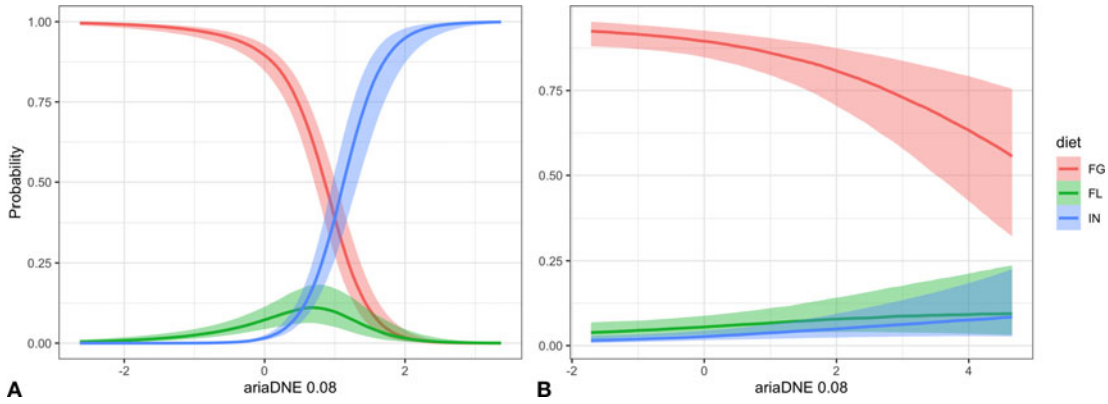

FIGURE 4. Relative probability of membership in each dietary category over the scaled range of values of ariaDNE bandwidth 0.08 evaluated alone on A, each tooth surface; and B, segmented tooth surfaces. Shaded area represents consistency interval of middle 95% of the mass of the posterior distribution.

other tooth cutting surfaces in both insectivores and folivores (Kay 1975; Yamashita 1998). However, leaves and insects differ in many important respects as potential food items.

Insect exoskeletons are both tough (requiring continuous application of force to propagate cracks) and stiff (requiring high concentrations of force to initiate cracks) (Strait 1993; Strait and Vincent 1998; Evans and Sanson 2003). The toughness of insect exoskeletons selects for the elaboration of blades, which can propagate cracks linearly and prevent the puncturing of a material without crack propagation, but the stiffness of exoskeletons selects for the development of blade edges and pointed cusps with minimal radius of curvature in three dimensions (Strait 1993; Evans and Sanson 2003). Animal matter is also highly elastic, which makes securing food items between interacting molar structures difficult, a problem best solved by high crests around deep basins (Strait 1997). Strepsirrhine insectivores appear to arrive at a morphological compromise by developing sharp cusps and narrow molar basins connected by sharp shearing crests. This occlusal topography is characterized by uniformly high curvature, yielding a high ariaDNE with low variance.

Leaves are also tough, but generally less stiff, with a planar geometry that minimizes the

TABLE 3. Reconstructions of dietary ecology in extinct strepsirrhines using discriminant function analysis (DFA). Reconstructed probabilities using genus means are reported, with the average reconstructions of all of the specimens in each genus reported in parentheses.

Group	Genus	Frugivory	Folivory	Insectivory	Godfrey et al. 2004; Marivaux et al. 2013; López-Torres et al. 2020
Archaeolemuridae	*Archaeolemur*	100% (85.1%)	0% (14.9%)	0% (0%)	Fruit, hard objects
	Hadropithecus	70.8% (62.6%)	29.1% (37.3%)	0% (0.17%)	Fruit, hard objects
Palaeopropithecidae	*Babakotia*	0% (5.9%)	100% (94.1%)	0% (0%)	Seed, fruit, foliage
	Mesopropithecus	98.7% (58.1%)	1% (28.2%)	003% (13.7%)	Seed, fruit, foliage
	Palaeopropithecus	0% (16.4%)	99.9% (83.4%)	0% (0.15%)	Seed, fruit, foliage
Megaladapidae	*Megaladapis*	80.2% (65.5%)	19.8% (33.3%)	0% (0.12%)	Leaves
Lemuridae	*Pachylemur*	100% (93.4%)	0.00% (3.41%)	0% (3.18%)	Fruit
Stem Strepsirrhini	*Djebelemur*	98% (60.5%)	0% (5.7%)	2% (33.8%)	Insects, fruit
Lorisiformes	*Karanisia*	97.7% (61.2%)	0.2% (38.4%)	0% (0.04%)	Fruit/gums
Lorisiformes	*Komba*	82.4% (23.5%)	0% (1.5%)	17.6% (75%)	NA
Lorisiformes	*Nycticeboides*	3.9% (30.1%)	93.4% (59.2%)	2.7% (10.7%)	NA
Chiromyiformes	*Plesiopithecus*	91.5% (70.5%)	8.5% (29.2%)	0% (0.03%)	Fruit
Chiromyiformes	*Propotto*	99.9% (86.2%)	0.01% (13.8%)	0% (0%)	NA
Lorisiformes	*Wadilemur*	99.5% (61%)	0% (8.2%)	0.04% (30.8%)	Fruit

https://doi.org/10.1017/pab.2021.9 Published online by Cambridge University Press

TABLE 4. Reconstructions of dietary ecology (means of the posterior probabilities distributions of likelihood of membership in each dietary category) in extinct strepsirrhines from Bayesian multilevel model.

Group	Genus	Frugivory	Folivory	Insectivory	Godfrey et al. 2004; Marivaux et al. 2013; López-Torres et al. 2020
Archaeolemuridae	*Archaeolemur*	72%	27.9%	0.1%	Fruit, hard objects
	Hadropithecus	64.6%	35%	3.7%	Fruit, hard objects
Palaeopropithecus	*Babakotia*	15.7%	84.3%	0%	Seed, fruit, foliage
	Mesopropithecus	64.9%	20.6%	14.5%	Seed, fruit, foliage
	Palaeopropithecus	45.5%	54.4%	0.01%	Seed, fruit, foliage
Megaladapidae	*Megaladapis*	70%	28.4%	1.4%	Leaves
Lemuridae	*Pachylemur*	76.9%	7.2%	15.9%	Fruit
Stem Strepsirrhini	*Djebelemur*	60.3%	1.9%	37.9%	Insects, fruit
Lorisiformes	*Karanisia*	61.1%	34.3%	4.6%	Fruit/gums
Lorisiformes	*Komba*	42.6%	0.4%	56.9%	NA
Lorisiformes	*Nycticeboides*	62.5%	32.6%	5%	NA
Chiromyiformes	*Plesiopithecus*	73.9%	25.8%	0.2%	Fruit
Chiromyiformes	*Propotto*	76.5%	22.8%	0.7%	NA
Lorisiformes	*Wadilemur*	59.6%	4.6%	35.8%	Fruit

ability for cracks to spread elastically through their tissue (Yamashita 1998; Lucas 2004; Ungar 2010). This combination of properties selects for the elaboration of elongated blades that interact to slice leaves and shallow basins against which leaves can be triturated (Yamashita 1998; Cuozzo and Yamashita 2006). The differences in curvature between open basins and high crests is captured by the relatively high CV of ariaDNE values across the tooth surfaces of folivores. Strepsirrhine folivores also develop multiple, intersecting blades that yield higher tooth surface complexity and a high OPC, as also observed in herbivorous rodents and carnivorans (Evans et al. 2007). Plants have evolved a range of adaptations to resist mammalian predation by increasing the rate of dental wear in leaf consumers (Vincent 1990; Lucas 2004; Ungar 2010). Strepsirrhine folivores appear to have adapted to resist this wear by increasing crown height, as captured by RFI (Boyer 2008; Pampush et al. 2016a).

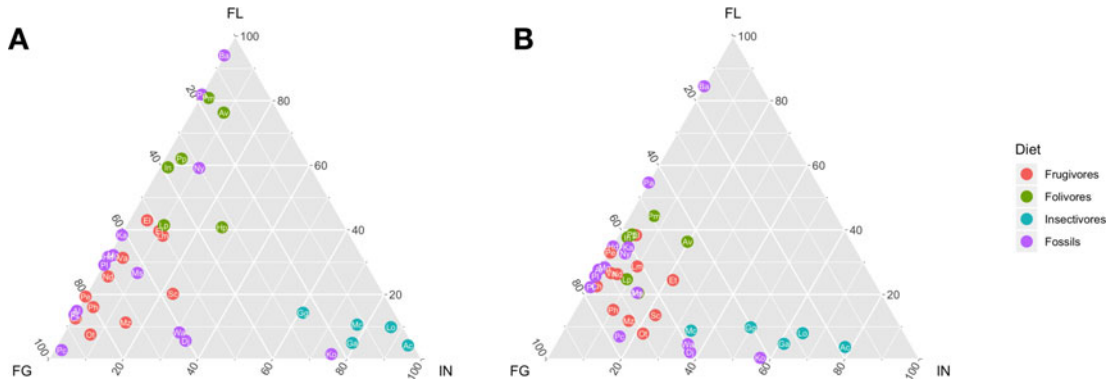

FIGURE 5. Ternary diagrams of the probability of reconstructed dietary ecologies from fossil and extant strepsirrhines. A, Dietary classification of each specimen averaged by genus, using discriminant function analysis (DFA) model incorporating ariaDNE 0.08, ariaDNE 0.08 coefficient of variation (CV), relief index (RFI), and orientation patch count (OPC); B, Dietary classification of each specimen averaged by genus, using Bayesian multilevel model incorporating ariaDNE 0.08, ariaDNE 0.08 CV, RFI, and OPC. FL, folivory; FG, frugivory; IN, insectivory. Ac, *Arctocebus*; Al, *Archaeolemur*; Av, *Avahi*; Ba, *Babakotia*; Ch, *Cheirogaleus*; Dj, *Djebelemur*; El, *Eulemur*; Et, *Euoticus*; Ga, *Galago*; Gg, *Galagoides*; Hd, *Hadropithecus*; Hp, *Hapalemur*; In, *Indri*; Ka, *Karanisia*; Ko, *Komba*; Lm, *Lemur*; Lo, *Loris*; Lp, *Lepilemur*; Mc, *Microcebus*; Mg, *Megaladapis*; Ms, *Mesopropithecus*; Mz, *Mirza*; Nd, *Nycticebus*; Ny, *Nycticeboides*; Ot, *Otolemur*; Pa, *Palaeopropithecus*; Pc, *Pachylemur*; Pe, *Perodicticus*; Ph, *Phaner*; Pl, *Plesiopithecus*; Pm, *Prolemur*; Pp, *Propithecus*; Pt, *Propotto*; Sc, *Sciurocheirus*; Va, *Varecia*; Wa, *Wadilemur*.

https://doi.org/10.1017/pab.2021.9 Published online by Cambridge University Press

Frugivores (which in this sample include gummivores) are thought to habitually consume foods with low toughness, although hard seed predation is important to some species (Godfrey et al. 2004; Lucas 2004; Ungar 2010). This lack of dietary structural carbohydrates is reflected in the low ariaDNE, ariaDNE CV, RFI, and OPC values characterizing frugivorous strepsirrhines in this sample. This supports the suggestion that the elaboration of shearing tooth structures is less important in processing diets characterized by lower levels of structural carbohydrates (Kay 1975; Bunn et al. 2011; Boyer 2008; Ungar 2010; Winchester et al. 2014).

The combination of Bayesian modeling and the use of explicit overfitting metrics largely supports the suitability of combinations of ariaDNE, RFI, and OPC for out-of-sample reconstruction. Metric comparisons supported the use of more highly parameterized models, in line with the multiproxy approach recommended by Pineda-Munoz et al. (2017). Models using disaggregated structures of the lower molar failed to outperform models constructed using ariaDNE values calculated for the whole surface. This suggests that, contrary to the concerns of Allen et al. (2015), tooth occlusal surfaces are under selection as integrated units for maximizing food fragmentation. Dental topography metrics calculated on occlusal surfaces do not appear to aggregate away dietary information reflected in disaggregated shearing crests, and instead may capture emergent properties of interacting tooth crown structures (Winchester 2016).

Genus mean and specimen-level DFA models suggest that a majority of the recently extinct subfossil lemur genera subsisted on fruits. It has been observed that lemur faunas are depauperate of frugivores when compared with similar primate communities on other landmasses (Ganzhorn 1992; Goodman and Ganzhorn 1997; Wright et al. 2005). This frugivore depauperate fauna may have resulted from the recent extinction of some large-bodied, specialized frugivores and hard-object feeders (especially the lemurid *Pachylemur* and the archaeolemurids *Archaeolemur* and *Hadropithecus*). The extinction of large-bodied frugivores would be consistent with a broader pattern of ecological contraction in lemur communities hypothesized to have occurred over the Quaternary (Godfrey et al. 2006, 2012).

Dietary reconstructions of subfossil lemurs using the all-parameters DFA models are largely consonant with reconstructions based on dental microwear and the elaboration of shearing quotients, both of which predict many subfossil lemur genera to have been frugivorous or hard-object feeding, with the exception of the sloth lemurs (Palaeopropithecidae) and *Megaladapis* (Jungers et al. 2002; Godfrey et al. 2004, 2006, 2012; Scott et al. 2009) (Fig. 6). Models reconstruct two of the sloth lemurs, *Palaeopropithecus* and *Babakotia*, as folivorous, as expected. The palaeopropithecid *Mesopropithecus*, however, seems aberrant in this regard, as its dietary ecology was reconstructed as frugivorous with relatively high confidence by DFA and Bayesian methods. Its molar structure resembles that of *Indri* and *Propithecus*, with ariaDNE and ariaDNE CV values most like *Propithecus*, both of which were reclassified as frugivorous by the Bayesian model (Table 5). *Propithecus* is known to exhibit a significant degree of seasonal diet switching toward fruits and seeds, and this ecology may have characterized *Mesopropithecus* or its ancestors (Godfrey et al. 2004; Norscia et al. 2006). The position of some paleopropithecids, although reconstructed as folivorous, far outside the ecological distribution of the extant species also underlines the extent to which some subfossil lemurs may lack clear ecological analogues among the extant fauna.

Both DFA and Bayesian models classified *Megaladapis* as frugivorous. This was surprising, as this taxon exhibits long shearing crests and a strongly folivorous microwear signal (Jungers et al. 2002; Godfrey et al. 2004). The signal for frugivory in *Megaladapis* seems to arise from its relatively low ariaDNE CV. The long, continuous crests displayed by *Megaladapis* molars may have lower variability in vertex bending than the shorter, intersecting crests of other lemur folivores. Sixty-six percent of specimens from the morphologically similar *Lepilemur* were also misclassified by the Bayesian model as frugivorous, suggesting that ariaDNE CV may struggle to characterize this dental configuration.

https://doi.org/10.1017/pab.2021.9 Published online by Cambridge University Press

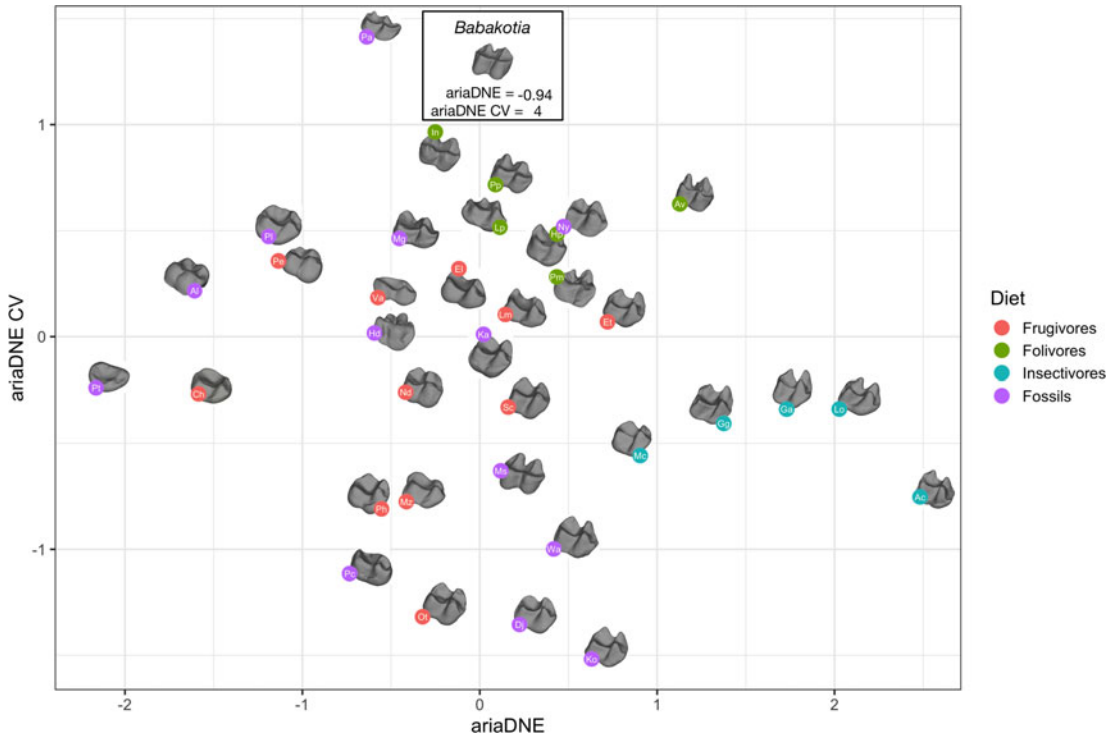

FIGURE 6. Strepsirrhine second molars plotted by scaled ariaDNE 0.08 and ariaDNE 0.08 coefficient of variation (CV) values. Ac, *Arctocebus*; Al, *Archaeolemur*; Av, *Avahi*; Ch, *Cheirogaleus*; Dj, *Djebelemur*; El, *Eulemur*; Et, *Euoticus*; Ga, *Galago*; Gg, *Galagoides*; Hd, *Hadropithecus*; Hp, *Hapalemur*; In, *Indri*; Ka, *Karanisia*; Ko, *Komba*; Lm, *Lemur*; Lo, *Loris*; Lp, *Lepilemur*; Mc, *Microcebus*; Mg, *Megaladapis*; Ms, *Mesopropithecus*; Mz, *Mirza*; Nd, *Nycticebus*; Ny, *Nycticeboides*; Ot, *Otolemur*; Pa, *Palaeopropithecus*; Pc, *Pachylemur*; Pe, *Perodicticus*; Ph, *Phaner*; Pl, *Plesiopithecus*; Pm, *Prolemur*; Pp, *Propithecus*; Pt, *Propotto*; Sc, *Sciurocheirus*; Va, *Varecia*; Wa, *Wadilemur*.

TABLE 5. Reconstructions of dietary ecology (means of the posterior probabilities distributions of likelihood of membership in each dietary category) in extant strepsirrhines from Bayesian multilevel model.

Group	Genus	Frugivory	Folivory	Insectivory	Diet
Lorisidae	*Arctocebus*	17.7%	3.8%	78.5%	Insectivory
	Loris	27.7%	8.2%	64.2%	Insectivory
	Nycticebus	68.3%	26.1%	5.7%	Frugivory
	Perodicticus	65.7%	33.6%	0.7%	Frugivory
Galagidae	*Euoticus*	54.3%	24.5%	21.2%	Frugivory
	Galago	33.7%	5%	61.2%	Insectivory
	Galagoides	41.1%	9.8%	49.1%	Insectivory
	Otolemur	69.4%	8%	22.7%	Frugivory
	Sciurocheirus	65.5%	13.1%	21.3%	Frugivory
Cheirogaleidae	*Cheirogaleus*	76.4%	21.5%	2.1%	Frugivory
	Microcebus	56.9%	8.6%	34.5%	Insectivory
	Mirza	72.3%	11.4%	16.3%	Frugivory
	Phaner	74.5%	15.1%	10.3%	Frugivory
Lepilemuridae	*Lepilemur*	66.6%	24.3%	9%	Folivory
Lemuridae	*Eulemur*	56.4%	38.8%	4.8%	Frugivory
	Hapalemur	65%	20.4%	14.5%	Folivory
	Lemur	60.6%	28.9%	10.5%	Frugivory
	Prolemur	49%	44.3%	6.7%	Folivory
	Varecia	69.9%	26.1%	3.9%	Frugivory
Indriidae	*Avahi*	43.8%	36.6%	19.6%	Folivory
	Indri	60.2%	37.1%	2.7%	Folivory
	Propithecus	57.8%	38.6%	3.7%	Folivory

https://doi.org/10.1017/pab.2021.9 Published online by Cambridge University Press

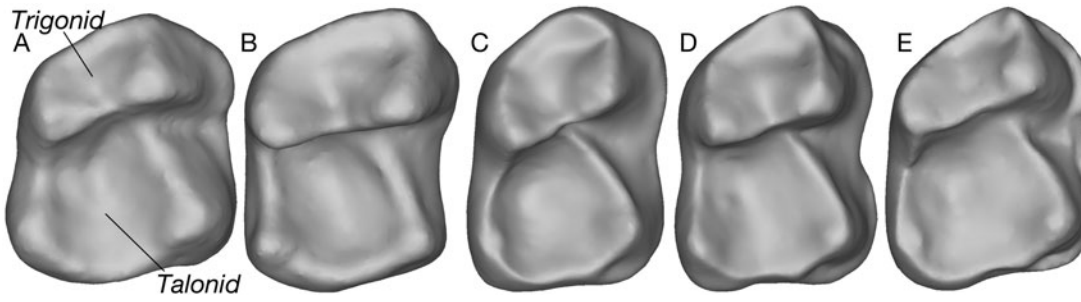

FIGURE 7. Occlusal view of the m2 of Paleogene strepsirrhines, *Microcebus*, and *Euoticus*. A, *Microcebus* (DLC 893m); B, *Euoticus* (MCZ 17591); C, *Djebelemur* (CBI 366); D, *Wadilemur* (DPC 16872); E, *Karanisia* (DPC 21456K).

Dental topography metrics were also applied to a sample of fossil strepsirrhines from the Paleogene and Neogene of Africa and Asia that includes a stem strepsirrhine, early fossil lorisiforms, and stem members of the chiromyiform lineage today represented by the aye-aye *Daubentonia*. Among these taxa, genus means strongly support frugivory (including potentially gummivory) in all taxa but *Nycticeboides* and *Komba*, with averaged specimen reclassifications indicating greater uncertainty but modally consistent results, despite the small size and apparently sharp teeth of *Djebelemur* and the Paleogene lorisiforms *Wadilemur* and *Karanisia* (Fig. 7). This is largely consistent with dietary reconstruction of the Paleogene species using shearing quotients (Kirk and Simons 2000; Marivaux et al. 2013).

The living mouse lemur *Microcebus*, which was reclassified by the DFA as an insectivore but by the Bayesian model as frugivorous, also consumes small fruits and gums, and would seem to represent the most likely ecological analogue for these early Paleogene taxa. However, *Microcebus* shows higher ariaDNE values than any of the three Paleogene genera (Fig. 8). This may capture the greater elaboration of flat trigonid and talonid basins in *Djebelemur* and *Wadilemur*, which could serve as crushing surfaces for processing small fruits, and the relatively high trigonid with low cusps of *Karanisia*. In these characters, these taxa seem to resemble the extant *Euoticus*, which is classified here as a frugivore/gummivore but is among the members of this category with the highest ariaDNE values. It seems likely that, like *Euoticus*, *Djebelemur*, *Karanisia*, and *Wadilemur* supplemented a frugivorous or gummivorous diet with insect protein. ariaDNE values from Paleogene fossil strepsirrhines overlap the distribution of both *Microcebus* and *Euoticus*, with a mean that is lower than both. The ecological distinction between small-bodied frugivore-insectivores and insectivore-frugivores may be ultimately difficult to detect using dental topographic analysis.

DFA, but not Bayesian, models reconstructed *Nycticeboides* as folivorous, a surprising result, as no extant lorisiforms consume leaves as a significant dietary component. *Nycticeboides*

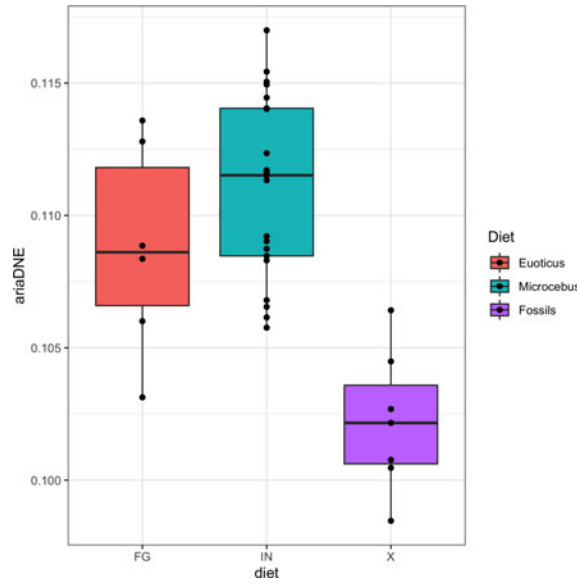

FIGURE 8. Box plot comparing specimen ariaDNE values of *Euoticus*, *Microcebus*, and Paleogene fossil taxa *Djebelemur*, *Karanisia*, and *Wadilemur*. IN, insectivory; FG, frugivory; X, unknown.

https://doi.org/10.1017/pab.2021.9 Published online by Cambridge University Press

shares with strepsirrhine folivores high ariaDNE CV, reflecting the development of sharp shearing crests and relatively flat basins. A qualitative description of the dentition of *Nycticeboides simpsoni* noted the development of shearing crests but argued against the likelihood that this taxon regularly consumed leaves due to its small size and phylogenetic bracketing (MacPhee and Jacobs 1986). Its body-size reconstruction is ambiguous, however, and it may have exceeded 500 g, placing it above "Kay's threshold," the approximate mass at which leaves become a more efficient source of dietary protein for primates than insects (Kay 1975; MacPhee and Jacobs 1986). This may indicate greater ecological diversity among Asian lorisiforms during the Miocene.

The reconstructed diets of Paleogene strepsirrhines suggest that adaptations for frugivory or gummivory among Eocene crown and near-crown (Djebelemurinae) strepsirrhines distinguished them ecologically from the more insectivorous *Afrotarsius* and folivorous adapiforms and anthropoids (Kirk and Simons 2000). The exploitation of angiosperm reproductive structures may have played a significant role in the early adaptive history of strepsirrhines in Afro-Arabia. As strepsirrhines expanded into habitats without incumbent primate insectivores (including Madagascar and South Asia), and after the extinction of mainland African insectivores like *Afrotarsius*, some strepsirrhine taxa apparently shifted into more specialist insectivore roles.

Acknowledgments

This paper emerged from a dissertation chapter to which G. Gunnell, R. Kay, D. McShea, E. St. Clair, C. Wall, and B. Williams gave helpful guidance. Helpful comments from N. Vitek, M. Silcox, and anonymous reviewer improved an earlier version of the article. Many undergraduates in the Boyer Lab also assisted in processing scans, especially K. Montane and M. Schaeffer. L. Godfrey, E. Seiffert, and the collections staff at the Smithsonian National Museum of Natural History, the American Museum of Natural History, the Field Museum of Natural History, the Natural History Museum (UK), and the Division of Fossil Primates at the Duke Lemur Center all provided valuable access to specimens. Funding was provided by the Duke Graduate School dissertation research domestic travel grant and summer research support and by the grants NSF BCS 1552848 to D.M.B., NSF BCS 130405 to D.M.B. and Elizabeth St. Clair, and NSF BCS 1825129 to D.M.B. and A. Harrington.

Data Availability Statement

Data available from the Dryad Digital Repository: https://doi.org/10.5061/dryad.4mw6m908m.

Literature Cited

Al-Aifari, R., I. Daubechies, and Y. Lipman. 2013. Continuous Procrustes distance between two surfaces. Communications on Pure and Applied Mathematics 66:934–964.

Allen, K.L., S. B. Cooke, L. A. Gonzales, and R. F. Kay. 2015. Dietary inference from upper and lower molar morphology in platyrrhine primates. PLoS ONE 10:e0118732.

Balko, E.A. 1998. A behaviorally plastic response to forest composition and logging disturbance by *Varecia variegata* in Ranomafana National Park, Madagascar. Ph.D. dissertation. Syracuse University, Syracuse, N.Y.

Bearder, S. K., and R. D. Martin. 1980. Acacia gum and its use by bushbabies, *Galago senegalensis* (Primates: Lorisidae). International Journal of Primatology 1:103–128.

Berthaume, M. A., J. Winchester, and K. Kupczik. 2019. Effects of cropping, smoothing, triangle count, and mesh resolution on 6 dental topographic metrics. PLoS ONE 14:e0216229.

Bhullar, B. A. S., A. R. Manafzadeh, J. A. Miyamae, E. A. Hoffman, E. L. Brainerd, C. Musinsky, and A. W. Crompton. 2019. Rolling of the jaw is essential for mammalian chewing and tribosphenic molar function. Nature 566:528–532.

Boyer, D. M. 2008. Relief index of second mandibular molars is a correlate of diet among prosimian primates and other euarchontan mammals. Journal of Human Evolution 55:1118–1137.

Britt, A., N. J. Randriamandratonirina, K. D. Glasscock, and B. R. Iambana. 2002. Diet and feeding behaviour of *Indri indri* in a low-altitude rain forest. Folia Primatologica 73:225–239.

Bunn, J. M., and P. S. Ungar. 2009. Dental topography and diets of four Old World monkey species. American Journal of Primatology 71:466–477.

Bunn, J. M., D. M. Boyer, Y. Lipman, E. M. St. Clair, J. Jernvall, and I. Daubechies. 2011. Comparing Dirichlet normal surface energy of tooth crowns, a new technique of molar shape quantification for dietary inference, with previous methods in isolation and in combination. American Journal of Physical Anthropology 145:247–261.

Bürkner, P. C. 2017. brms: an R package for Bayesian multilevel models using Stan. Journal of Statistical Software 80:1–28.

Bürkner, P. C. 2020. Estimating phylogenetic multilevel models with brms. https://cran.r-project.org/web/packages/brms/vignettes/brms_phylogenetics.html, accessed 7 January 2021.

Burrows, A. M., and L. T. Nash. 2010. Searching for dental signals of exudativory in Galagos. Pp. 211–233 *in* A. M. Burrows and L. T. Nash, eds. The evolution of exudativory in primates. Springer, New York.

Charles-Dominique, P. 1977. Ecology and behaviour of nocturnal primates: prosimians of equatorial West Africa. Columbia University Press, New York.

https://doi.org/10.1017/pab.2021.9 Published online by Cambridge University Press

Charles-Dominique, P. 1979. Field studies of lorisid behavior: methodological aspects. Study of Prosimian Behavior. Academic Press, Cambridge, Mass.

Crompton, A. W. 1970. Functional significance of the therian molar pattern. Nature 227:197–199.

Cuozzo, F. P., and N. Yamashita. 2006. Impact of ecology on the teeth of extant lemurs: a review of dental adaptations, function, and life history. Pp. 67–96 *in* L. Gould and M. L. Sauther, eds. Lemurs: ecology and adaptation. Springer, New York.

Dammhahn, M., and P. M. Kappeler 2008. Small-scale coexistence of two mouse lemur species (*Microcebus berthae* and *M. murinus*) within a homogeneous competitive environment. Oecologia 157:473–483.

Erhart, E. M., S. R. Tecot, and C. Grassi. 2018. Interannual variation in diet, dietary diversity, and dietary overlap in three sympatric strepsirrhine species in southeastern Madagascar. International Journal of Primatology 39:289–311.

Evans, A. R. 2013. Shape descriptors as ecometrics in dental ecology. Hystrix: Italian Journal of Mammalogy 24:133–140.

Evans, A. R., and J. Jernvall. 2009. Patterns and constraints in carnivoran and rodent dental complexity and tooth size. Journal of Vertebrate Paleontology 29:24A.

Evans, A. R., and S. Pineda-Munoz. 2018. Inferring mammal dietary ecology from dental morphology. Pp. 37–51 *in* D. A. Croft, D. Su, and S. W. Simpson, eds. Methods in paleoecology. Springer, New York.

Evans, A. R., and Sanson, G. D. 2003. The tooth of perfection: functional and spatial constraints on mammalian tooth shape. Biological Journal of the Linnean Society 78:173–191.

Evans, A. R., G. P. Wilson, M. Fortelius, and J. Jernvall. 2007. High-level similarity of dentitions in carnivorans and rodents. Nature 445:78–81.

Fietz, J., and J. U. Ganzhorn. 1999. Feeding ecology of the hibernating primate *Cheirogaleus medius*: how does it get so fat? Oecologia 121:157–164.

Fortelius, M., J. Eronen, J. Jernvall, L. Liu, D. Pushkina, J. Rinne, A. Tesakov, I. Vislobokova, Z. Zhang, and L. Zhou. 2002. Fossil mammals resolve regional patterns of Eurasian climate change over 20 million years. Evolutionary Ecology Research 4:1005–1016.

Ganzhorn, J. U. 1992. Leaf chemistry and the biomass of folivorous primates in tropical forests. Oecologia 91:540–547.

Ganzhorn, J. U., J. P. Abraham, and M. Razanahoera-Rakotomalala. 1985. Some aspects of the natural history and food selection of *Avahi laniger*. Primates 26:452–463.

Gao, T. 2015. Hypoelliptic diffusion maps and their applications in automated geometric morphometrics. Ph.D. thesis. Duke University, Durham, N.C.

Gao, T. 2021. The diffusion geometry of fibre bundles: horizontal diffusion maps. Applied and Computational Harmonic Analysis 50:147–215.

Gao T., G. S. Yapuncich, I. Daubechies, S. Mukherjee, and D. M. Boyer. 2018. Development and assessment of fully automated and globally transitive geometric morphometric methods, with application to a biological comparative dataset with high interspecific variation. Anatomical Record 301:636–658.

Godfrey, L. R. 2017. Subfossil lemurs. *In* A. Fuentes *et al.*, eds. The international encyclopedia or primatology. Wiley, New York.

Godfrey, L. R., G. M. Semprebon, W. L. Jungers, M. R. Sutherland, E. L. Simons, and N. Solounias. 2004. Dental use wear in extinct lemurs: evidence of diet and niche differentiation. Journal of Human Evolution 47:145–169.

Godfrey, L. R., G. M. Semprebon, G. T. Schwartz, W. L. Jungers, E. K. Flanagan, F. P. Cuozzo, and S. J. King. 2005. New insights into old lemurs: the tropic adaptations of the Archaeolemuridae. International Journal of Primatology 26:825–854.

Godfrey, L. R., W. L. Jungers, and G. T. Schwartz. 2006. Ecology and extinction of Madagascar's subfossil lemurs. Pp. 41–64 *in* L. Gould and M. L. Sauther, eds. Lemurs: ecology and adaptation. Springer, New York.

Godfrey, L. R., J. M. Winchester, S. J. King, D. M. Boyer, and J. Jernvall. 2012. Dental topography indicates ecological contraction of lemur communities. American Journal of Physical Anthropology 148:215–227.

Godfrey, L. R., R. E. Crowley, K. M. Muldoon, E. A. Kelley, S. J. King, A. W. Best, and A. Berthaume. 2016. What did *Hadropithecus* eat, and why should palaeoanthropologists care? American Journal of Primatology 78:1098–1112.

Goodman, S. M., and J. U. Ganzhorn. 1997. Rarity of figs (*Ficus*) on Madagascar and its relationship to a depauperate frugivore community. Revue d'Ecologie 52:321–329.

Gould, L. 2006. *Lemur catta* ecology: what we know and what we need to know. Pp. 255–274 *in* L. Gould and M. L. Sauther, eds. Lemurs: ecology and adaptation. Springer, New York.

Gregory, W. K. 1922. Origin and evolution of the human dentition. Williams and Wilkins, Baltimore.

Harcourt, C. 1986. Seasonal variation in the diet of South African galagos. International Journal of Primatology 7:491–506.

Harcourt, C. 1991. Diet and behaviour of a nocturnal lemur, *Avahi laniger*, in the wild. Journal of Zoology 223:667–674.

Harcourt, C. S., and L. T. Nash. 1986. Species differences in substrate use and diet between sympatric galagos in two Kenyan coastal forests. Primates 27:41–52.

Hemingway, C. A. 1996. Morphology and phenology of seeds and whole fruit eaten by Milne-Edwards' sifaka, *Propithecus diadema edwardsi*, in Ranomafana National Park, Madagascar. International Journal of Primatology 17:637–659.

Herrera, J. P., and L. M. Dávalos. 2016. Phylogeny and divergence times of lemurs inferred with recent and ancient fossils in the tree. Systematic Biology 65:772–791.

Hladik, C. M. 1979. Diet and ecology of prosimians. Pp. 307–357 *in* G. A. Doyle, ed. Study of prosimian behavior. Academic Press, Cambridge, Mass.

Hladik, C. M., P. Charles-Dominique, and J. J. Petter. 1980. Feeding strategies of five nocturnal prosimians in the dry forest of the west coast of Madagascar. Pp. 41–73 *in* P. Charles-Dominique, ed. Nocturnal Malagasy primates: ecology, physiology, and behaviour. Academic Press, Cambridge, Mass.

Housworth, E. A., E. P. Martins, and M. Lynch. 2004. The phylogenetic mixed model. American Naturalist 163:84–96.

Jardine, P. E., C. M. Janis, S. Sahney, and M. J. Benton. 2012. Grit not grass: concordant patterns of early origin of hypsodonty in Great Plains ungulates and Glires. Palaeogeography, Palaeoclimatology, and Palaeoecology 365:1–10.

Jungers, W. L., L. R. Godfrey, E. L. Simons, R. E. Wunderlich, B. G. Richmond, and P. S. Chatrath. 2002. Ecomorphology and behavior of giant extinct lemurs from Madagascar. Pp. 371–411 *in* J. Plavcan, R. F. Kay, W. Jungers, and C. P. van Schaik, eds. Reconstructing behavior in the primate fossil record. Springer, New York.

Kay, R. F. 1975. The functional adaptations of primate molar teeth. American Journal of Physical Anthropology 43:195–215.

Kay, R. F. 1977. The evolution of molar occlusion in the Cercopithecidae and early catarrhines. American Journal of Physical Anthropology 46:327–352.

Kay, R. F. 1978. Molar structure and diet in extant Cercopithecidae. Pp. 309–339 *in* M. F. Teaford, M. M. Smith, and M. W. J. Ferguson, eds. Development, function, and evolution of teeth. Academic Press, New York.

Kay, R. F., and H. H. Covert. 1984. Anatomy and behaviour of extinct primates. Pp. 467–508 *in* D. J. Chivers, B. A. Wood, and A. Bilsborough, eds. Food acquisition and processing in primates. Springer, New York.

Kay, R. F., and K. M. Hiiemae. 1974. Jaw movement and tooth use in recent and fossil primates. American Journal of Physical Anthropology 40:227–256.

Kay, R. F., and W. L. Hylander. 1978. The dental structure of mammalian folivores with special reference to Primates and Phalangeroidea (Marsupialia). Pp. 173–191 *in* G. G. Montgomery, ed. The ecology of arboreal folivores. Smithsonian Institution Press, Washington, D.C.

Kay, R. F., and E. L. Simons. 1980. The ecology of Oligocene African Anthropoidea. International Journal of Primatology 1:21–37.

Kay, R. F., and P. S. Ungar. 1997. Dental evidence for diet in some Miocene catarrhines with comments on the effects of phylogeny on the interpretation of adaptation. Pp. 131–151 *in* D. R. Begun, C. V. Ward, and M. D. Rose, eds. Function, phylogeny, and fossils. Springer, New York.

Kirk, E. C., and E. L. Simons. 2000. Diets of fossil primates from the Fayum Depression of Egypt: a quantitative analysis of molar shearing. Journal of Human Evolution 40:203–229.

Lahann, P. 2007. Feeding ecology and seed dispersal of sympatric cheirogaleid lemurs (*Microcebus murinus*, *Cheirogaleus medius*, *Cheirogaleus major*) in the littoral rainforest of south-east Madagascar. Journal of Zoology 271:88–98.

López-Torres, S., Keegan, S. R., Prufrock K. A., Lin, D., and Silcox, M. T. 2017. Dental topographic analysis of paromomyid (Plesiadapiformes, Primates) cheek teeth: more than 15 million years of changing surfaces and shifting ecologies. Historical Biology 30(1–2):76–88.

López-Torres, S., K. R. Selig, A. M. Burrows, and M. T. Silcox. 2020. The toothcomb of *Karanisia clarki*: was this species an exudate-feeder? Pp. 67–75 *in* K. A.-I. Nekaris and A. M. Burrows, eds. Ecology and conservation of lorises and pottos. Cambridge University Press, Cambridge.

Lucas, P. W. 2004. Dental functional morphology: how teeth work. Cambridge University Press, Cambridge.

MacPhee, R. D. E., and L. L. Jacobs. 1986. *Nycticeboides simpsoni* and the morphology, adaptations, and relationships of Miocene Siwalik Lorisidae. Contributions to Geology, University of Wyoming Special Paper 3:131–161.

Marivaux, L., A. Ramdarshan, E. M. Essid, and W. Marzougui, H. K. Ammar, R. Lebrun, B. Marandat, G. Merzeraud, R. Tabuce, and M. Vianey-Liaud. 2013. *Djebelemur*, a tiny pre-tooth-combed primate from the Eocene of Tunisia: a glimpse into the origin of crown strepsirrhines. PLoS ONE 9:e80778.

Masters, J. C., W. H. R. Lumsden, and D. A. Young. 1988. Reproductive and dietary parameters in wild greater galago populations. International Journal of Primatology 9:573–592.

Masters, J. C., F. Génin, S. Couette, C. P. Groves, S. D. Nash, M. Delpero, and L. Pozzi. 2017. A new genus for the eastern dwarf galagos (Primates: Galagidae). Zoological Journal of the Linnaean Society 181:229–241.

McCrossin, M. L. 1992. New species of bushbaby from the Middle Miocene of Maboko Island, Kenya. American Journal of Physical Anthropology 89:215–233.

McElreath, R. 2015. Statistical rethinking: a Bayesian course with examples in R and Stan. Chapman and Hall/CRC, New York.

Nash, L. T. 1986. Dietary, behavioral, and morphological aspects of gummivory in primates. American Journal of Physical Anthropology 29:113–137.

Nekaris, K. A. I. 2005. Foraging behaviour of the slender loris (*Loris lydekkerianus lydekkerianus*): implications for theories of primate origins. Journal of Human Evolution 49:289–300.

Nekaris, K. A. I., and D. T. Rasmussen. 2003. Diet and feeding behavior of Mysore slender lorises. International Journal of Primatology 24:33–46.

Norscia, I., V. Carrai, and S. M. Borgognini-Tarli. 2006. Influence of dry season and food quality and quantity on behavior and feeding strategy of *Propithecus verreauxi* in Kirindy, Madagascar. International Journal of Primatology 27:1001–1022.

Olson, E. R., R. A. Marsh, B. N. Bovard, H. L. Randrianarimanana, M. Ravaloharimanitra, J. H. Ratsimbazafy, and T. King. 2013. Habitat preferences of the critically endangered greater bamboo lemur (*Prolemur simus*) and densities of one of its primary food sources, Madagascar giant bamboo (*Cathariostachys madagascariensis*), in sites with different degrees of anthropogenic and natural disturbance. International Journal of Primatology 34:486–499.

Overdorff, D. J. 1992. Differential patterns in flower feeding by *Eulemur fulvus rufus* and *Eulemur rubriventer* in Madagascar. American Journal of Primatology 28:191–203.

Overdorff, D. J., S. G. Strait, and A. Telo. 1997. Seasonal variation in activity and diet in a small-bodied folivorous primate, *Hapalemur griseus*, in southeastern Madagascar. American Journal of Primatology 43:211–223.

Pampush, J. D., J. P. Spradley, P. E. Morse, A. R. Harrington, K. L. Allen, D. M. Boyer, and R. F. Kay. 2016a. Wear and its effects of dental topography measures in howling monkeys (*Alouatta palliata*). American Journal of Physical Anthropology 161:705–721.

Pampush, J. D., J. M. Winchester, P. E. Morse, A. Q. Vining, D. M. Boyer, and R. F. Kay. 2016b. Introducing molaR: a new R package for quantitative topographic analysis of teeth (and other topographic surfaces). Journal of Mammalian Evolution 23:397–412.

Patel, B. A., D. M. Boyer, B. A. Perchalski, T. M. Ryan, E. M. St. Clair, J. M. Winchester, and E. R. Seiffert. 2017. New fossils and the paleobiology of *Karanisia clarki* from the late Eocene of Egypt. American Journal of Physical Anthropology 162:310–311.

Pineda-Munoz, S., I. A. Lazagabaster, J. Alroy, and A. R. Evans. 2017. Inferring diet from dental morphology in terrestrial mammals. Methods in Ecology and Evolution 8:481–491.

Powzyk, J. A., and C. B. Mowry. 2003. Dietary and feeding differences between sympatric *Propithecus diadema diadema* and *Indri indri*. International Journal of Primatology 24:1143–1162.

Rode-Margono, E. J., V. Nijman, N. K. Wirdateti, and K. A. I. Nekaris. 2014. Ethology of the critically endangered Javan slow loris *Nycticebus javanicus* E. Geoffroy Saint-Hilaire in West Java. Asian Primates 4:27–41.

Sato, H., L. Santini, E. R. Patel, M. Campera, N. Yamashita, I. C. Colquhoun, and G. Donati. 2016. Dietary flexibility and feeding strategies of *Eulemur:* a comparison with *Propithecus*. International Journal of Primatology 37:109–129.

Scott, J. R., L. R. Godfrey, W. L. Jungers, R. S. Scott, E. L. Simons, M. F. Teaford, P. S. Ungar, and A. Walker. 2009. Dental microwear texture analysis of two families of subfossil lemurs from Madagascar. Journal of Human Evolution 56:405–416.

Selig, R. S., E. J. Sargis, and M. T. Silcox. 2019. The frugivorous insectivores? Functional morphological analysis of molar topography for inferring diet in extant treeshrews (Scandentia). Journal of Mammalogy 100:1901–1917.

Shan, S., S. Z. Kovalsky, J. M. Winchester, D. M. Boyer, and I. Daubechies. 2019. aria DNE: a robustly implemented algorithm for Dirichlet energy of the normal. Methods in Ecology and Evolution 10:541–552.

Sheine, W. S., and R. F. Kay. 1982. A model for comparison of masticatory effectiveness in primates. Journal of Morphology 172:139–149.

Simpson, G. G. 1933. Paleobiology of Jurassic mammals. Palaeobiologica Band V.

Spagnolo, S. 1976. Convergence in energy for elliptic operators. *In* B. Hubbard, ed. Numerical solution of partial differential equations III:469–499. Elsevier, New York.

Spradley, J. P., J. D Pampush, P. E. Morse, and R. F. Kay. 2017. Smooth operator: the effects of different 3D mesh retriangulation protocols on the computation of Dirichlet normal energy. American Journal of Physical Anthropology 163:94–109.

Sterling, E. J., E. S. Dierenfeld, C. J. Ashbourne, and A. T. Feistner. 1994. Dietary intake, food composition and nutrient intake in wild and captive populations of *Daubentonia madagascariensis*. Folia Primatologica (Basel) 62:115–124.

Strait, S. G. 1993. Differences in occlusal morphology and molar size in frugivores and faunivores. Journal of Human Evolution 25:471–484.

Strait, S. G. 1997. Tooth use and the physical properties of food. Evolutionary Anthropology 5:199–211.

Strait, S. G., and J. F. V. Vincent. 1998. Primate faunivores: physical properties of prey items. International Journal of Primatology 19:867–878.

Streicher, U. 2004. Aspects of the ecology and conservation of the pygmy loris *Nycticebus pygmaeus* in Vietnam. Ph.D. thesis. Ludwig Maximilians Universität, Munich.

Streicher, U. 2009. Diet and feeding behaviour of pygmy lorises (*Nycticebus pygmaeus*) in Vietnam. American Journal of Primatology 3:37–44.

Thalmann, U. 2001. Food resource characteristics in two nocturnal lemurs with different social behavior: *Avahi occidentalis* and *Lepilemur edwardsi*. International Journal of Primatology 22:287–324.

Ungar, P. S. 2007. Dental functional morphology. Pp. 39–55 *in* P. S. Ungar, ed. Evolution of the human diet: the known, the unknown, and the unknowable. Oxford University Press, Oxford.

Ungar, P. S. 2010. Mammal teeth: origin, evolution, and diversity. Johns Hopkins University Press, Baltimore.

Ungar, P. S., and M. Williamson. 2000. Exploring the effects of tooth wear on functional morphology: a preliminary study using dental topographic analysis. Palaeontologia Electronica 3:1–18.

Vasey, N. 2000. Niche separation in *Varecia variegata rubra* and *Eulemur fulvus albifrons*: I. Interspecific patterns. American Journal of Physical Anthropology 112:411–431.

Vasey, N. 2002. Niche separation in *Varecia variegata rubra* and *Eulemur fulvus albifrons*: II. Intraspecific patterns. American Journal of Physical Anthropology 118:169–183.

Vehtari, A., A. Gelman, and J. Gabry. (2017) Practical Bayesian model evaluation using leave-one-out cross-validation and WAIC. Statistics and Computing 27:1413–1432.

Vincent, J. 1990. Structural biomaterials. Princeton University Press, Princeton, N.J.

Walker, A. 1969. True affinities of *Propotto leakeyi* Simpson 1967. Nature 223:647–648.

Wiens, F., A. Zitzmann, and N. A. Hussein. 2006. Fast food for slow lorises: is low metabolism related to secondary compounds in high-energy plant diet? Journal of Mammalogy 87:790–798.

Winchester, J. M. 2016. MorphoTester: an open source application for morphological topographic analysis. PLoS ONE 11:e0147649.

Winchester, J. M. 2020. hecate. https://github.com/JuliaWinchester/hecate, accessed 10 March 2020.

Winchester, J. M., D. M. Boyer, E. M. St. Clair, and A. D. Gosselin-Ildari, S. B. Cooke, and J. A. Ledogar. 2014. Dental topography of platyrrhines and prosimians: convergence and contrasts. American Journal of Physical Anthropology 153:29–44.

Wright, P. C., V. R. Razafindratsita, S. T. Pochron, and J. Jernvall. 2005. The key to Madagascar frugivores. Pp. 121–138 *in* J. L. Dew, and J. P Boubli, eds. Tropical fruits and frugivores. Springer, New York.

Yamashita, N. 1998. Functional dental correlates of food properties in five Malagasy lemur species. American Journal of Physical Anthropology 106:169–188.

Yamashita, N. 2003. Food procurement and tooth use in two sympatric lemur species. American Journal of Physical Anthropology 121:125–133.

https://doi.org/10.1017/pab.2021.9 Published online by Cambridge University Press